Design of Unimodular Sequence with Good Correlation and Spectral Stopband

Laibao Cao[1,a], Dexing Li[1,b], Kai Zhou[1,c], Chunlin Huang[1,d], Tao Liu[1,e], and Cheng Chen[1,f]

[1]School of Eletronic Science and Technology National University of Defense Technology Changsha, 410073, China
a. caolaibao@nudt.edu.cn, b. ldx 02071462@163.com, c. zhoukai15@nudt.edu.cn
d. hclg@163.com, e. liutao.apo@gmail.com, f. cc233cc@foxmail.com.

Keywords: Unimodular sequence design, spectral stopband, integrated sidelobe level (ISL), alternating direction method of multipliers (ADMM), truncated singular value decomposition (TSVD).

Abstract: Recently, unimodular sequence with good correlation and stopband has attracted considerable attention because it not only benefits the suppression of range sidelobe but also helps to avoid narrowband interference and electronic jamming. In this paper, an algorithm is proposed to design sequence with suppressed integrated sidelobe level (ISL) and stopband power spectrum density based on alternating direction method of multipliers (ADMM). The design problem is formulated as constrained bi-objective optimization problem. By applying the Pareto optimization framework and parallelogram identity, the metric is rewritten as sum of two quadratic functions. The optimization problem is further simplified as quadratically constrained linear program and linearly constrained quadratic program via variable separation. The simplified optimization problem is then solved by ADMM. Additionally, the computation complexity is reduced in the most computationally demanding step based on truncated singular value decomposition (TSVD) and fast Fourier transform (FFT). The numerical simulations demonstrate the effectiveness of the proposed algorithms.

1. Introduction

As the amount of radars and communication electronics grows, the number of consecutive bands that radars can utilize is decreasing. For instance, radar signal should reduce interference over the existing navigation and tele- communication systems [1]. The transmitted signal should also avoid certain bands that exist strong narrowband interference and electronic jamming [2]. Thus, it is required to design sequence with stopband, namely low power spectrum density in certain band. However, spectral stopband may degrade the performance of autocorrelation sidelobe, e.g. waveform with spectral stopband may have higher peak sidelobe level (PSL) and integrated sidelobe level (ISL) than those without spectral stopband [3]. It is a challenging problem to design sequence with stopband while maintaining good autocorrelation, especially when unimodular constraint is considered.

To date, several studies have investigated to design unimodular sequence with stopband and good correlation. Overall, these studies are classified into two main categories. The first category tackles the design problem by optimizing the frequency-modulated waveforms. For example, spectral nulling technology is implemented in frequency modulation to design waveform with spectral stopband [4]. Deep spectral nulls can be produced at spectral sidelobes by introducing a small time-varying phase offset [5]. However, they both suffer high autocorrelation sidelobes because the correlation metrics are not taken into consideration. Recently, [6] and [7] propose polyphase coded FM (PCFM) waveform that is constant envelope and spectrally well contained. To design sequences with good spectral compatibility and correlation performance, a gradient descent-based method was proposed which follow the PCFM design scheme [8].

The second category addresses the design problem by optimizing phase coding sequence. For instance, based on fast Fourier transform (FFT) operations, SCAN algorithm is proposed to suppress stopband spectral power and ISL under the peak-to-average power ratio (PAR) constraint [2], [9]. In [10], phase-only sequence with desired correlation and stopband properties was designed based on pattern search. Algorithm based on majorization-minimization was proposed in [11] to design spectrally constrained sequence with low autocorrelation sidelobes (hereinafter referred to as SMISL). A method of designing sparse frequency waveform with sidelobe constraint is reported based on ambiguity function theory [12]. Algorithms based on majorization-minimization and a gradient method were derived to suppressed autocorrelation sidelobes and arbitrary frequency stopband [13]. In addition, several studies were reported to design sequences with spectral shape be closer to desired shape and low mask [14]-[17].

Waveform design is usually subject to several constraints, e.g. modular constraint, similarity constraint, energy constraint and ambiguity function constraint [1], [18], [19]. Unimodular constraint is often taken into consideration in order to avoid signal distortion and energy loss caused by the nonlinear radio frequency component [20]. Peak-to-average ratio constraints is a more general modular constraint than unimodular constraint [21]. Similarity constraint is needed to force the designed sequences to share good properties of the reference sequence, e.g. the ambiguity function [22], [23]. In addition, energy constraint is also considered due to the limitation of power amplifier in the practice. All of the constraints are significant in practice, and are widely considered in radar waveform design field.

The aforementioned SCAN and SMISL [9], [11] have fast convergence, low computational complexity, and suppressed ISL and stopband power. However, both algorithms suffer poor correlation performance due to high PSL. Besides, the sequences designed by SMISL have high spectral jitter which may cause peak stopband power (Pstop). Alternating direction method of multipliers (ADMM) has advantage of handling objective functions completely separately and finding global optimal solution [24]. It has been widely used in waveform design for optimization of radar transmit beampattern [25], signal-to-interference-plus-noise ratio [19], and correlation sidelobe level [16]. To suppress the correlation sidelobe level and stopband spectral power simultaneously, the ADMM is introduced to the design of phase coding sequence under unimodular constraint.

In this paper, we focus on the correlation sidelobe level and power spectrum density minimization-based unimodular sequence design. Firstly, we establish the design problem formulation based on Pareto optimization, and formulate the bi-objective optimization problem as a single objective optimization problem. The penalty function is then reformulated as an equivalent quadratic function based on parallelogram identity. The nonconvex problem is further simplified as sum of linear and quadratic components by introducing auxiliary variables, which is solved by ADMM. Different from [16], an efficient method is proposed based on truncated singular value decomposition (TSVD) [26], [27] and fast Fourier transform (FFT) in the most computationally

demanding step, where a vast number of computations are required by matrix inverse and multiplication. Numerical simulations demonstrate the effectiveness of the proposed algorithm, and the superiority of the proposed algorithm over state-of-the-art methods in terms of PSL while maintaining the same ISL.

The structure of the paper is as follows. Section I presents a brief introduction to the unimodular waveform design with good correlation and spectral stopband. Section II formulates the designing problem considered in this paper. Section III illustrates the reformulation of the design problem and details of the proposed algorithm. Section IV performs several numerical simulations compared with the state-of-the-art algorithms to validate the effectiveness of proposed algorithm. Section V summarizes the conclusions of the paper including a discussion on future research.

Notation: We use boldface upper case letters for matrix and boldface lower case letters for column vectors. The $|\cdot|$, $\|\cdot\|_2$ and $\|\cdot\|_F$ represent the absolute value of complex valued scalar, Euclidean norm of vector and Frobenius norm of matrix, respectively. $(\cdot)^T$ is transpose and $(\cdot)^H$ is Hermitian transpose. $(\cdot)^*$ represents the complex conjugate of vector. $\Re(\cdot)$ and $\Im(\cdot)$ denote the real and imaginary parts of complex-valued scalar, vector and matrix. $diag(\cdot)$ denotes a square diagonal matrix with the elements of a given vector on the main diagonal.

2. Problem formulation

In this section, we formulate the problem of designing sequence with good autocorrelation and spectral stopband. Firstly, we formulate the problem of suppressing to correlation sidelobe. Let ,denote the aperiodic unimodular sequence of length N to be designed. The aperiodic autocorrelation function associated with x is defined as.

$$r(k)=\sum_{n=k+1}^{N} x(n)x^*(n-k)=r*(-k),k=0,1,\cdots N-1 \tag{1}$$

Peak sidelobe level (PSL) and ISL are usually used for synthesizing sequence with good correlation. The PSL metric is typically formulated as the infinite norm of $\{r(k)\}_{k=1}^{N}$, and is difficult to optimize directly. In this paper, we focus on the optimization of ISL metric, which can be written as Euclidean norm of $\{r(k)\}_{k=1}^{N}$, namely, the sum of the squares of $\{r(k)\}_{k=1}^{N}$.

$$f_{ISL}(x)=2\sum_{k=1}^{N-1}|r(k)|^2 \tag{2}$$

As shown in (1) and (2), the ISL metric is a quartic function with respect to variable x, which is usually difficult to solving directly due to the non-convexity. With the use of Parseval-type equality, completeness of Euclidean space and the continuity of Euclidean norm, the minimization of ISL is almost equivalent to the following ISL metric in the frequency domain (readers can refer to [2], [28], [29] for more details).

$$f_{ISL}(x)=\sum_{p=1}^{2N}\left|g_p^H \mathrm{x}-\sqrt{N}e^{j\varphi_p}\right|^2 \tag{3}$$

where $g_p^H=[e^{-j\omega_p},e^{-j\omega_p 2},\cdots,e^{-j\omega_p N}]$ is the DFT vector, and ω_p is given by

$$\omega_p=\frac{2\pi}{2N}p, p=0,1,\cdots,2N-1 \tag{4}$$

Let G^H be the first N columns of the 2N×2N DFT matrix given by

$$G^H = \begin{bmatrix} g_0^H \\ g_1^H \\ \vdots \\ g_{2N-1}^H \end{bmatrix} \tag{5}$$

Let $\mathbf{v}$ be an auxiliary variable defined as $v = [e^{j\varphi_1}, e^{j\varphi_2}, \cdots e^{j\varphi_{2N}}]^T \in C^{2N-1}$. The ISL metric is then

$$f_{ISL}(x) = \left\| G^H \mathrm{x} - \sqrt{N}\mathrm{v} \right\|^2 \tag{6}$$

Secondly, we consider the formulation of spectral stopband suppression. By choosing the frequency grid as 1/2N, the normalized frequency set can be defined as $\{p/2N\}_{p=0}^{2N-1}$, which can be denoted by the set of indices $\Omega = [0,1,\cdots,2N-1]$ Spectral stopband requires that the power distributed in the specified set of frequencies should be suppressed. Suppose that Ω_S is the set of frequencies $\Omega_S = [N_a,\cdots,N_b]$ should be avoided, denoted hereinafter by the set of indices $2N \times N$ We form an matrix $\mathbf{S}^H$ from $\mathbf{G}^H$ given by

$$\mathbf{S}^H = \begin{bmatrix} 0 \\ \vdots \\ \mathbf{g}_{N_a}^H \\ \vdots \\ \mathbf{g}_{N_b}^H \\ \vdots \\ 0 \end{bmatrix} \tag{7}$$

The stopband power can be suppressed by minimizing the following penalty function.

$$f_{SP}(\mathbf{x}) = \left\| \mathbf{S}^H \mathrm{x} \right\|^2 \tag{8}$$

Finally, we focus on the formulation of designing unimodular sequences with suppressed autocorrelation sidelobe and stopband power. The design problem can be formulated as bi-objective optimization problem under unimodular constraint.

$$\begin{aligned} &\min f_{ISL}(\mathbf{x}), f_{SP}(\mathbf{x}) \\ s.t. \quad &\left|\mathbf{x}(n)\right| = 1, n = 1,2,\cdots,N. \\ &\left|\mathbf{v}(n)\right| = 1, n = 1,2,\cdots,2N. \end{aligned} \tag{9}$$

In the bi-objective optimization framework, it is hard to find optimal solution minimizing two penalty functions simultaneous [30]. To find the optimal solution of (9), the Pareto optimization method is implemented in this paper. Let Pareto weight $\varepsilon \in [0,1]$, the optimization problem is then

$$\begin{aligned} &\min \left\{ \varepsilon f_{SP}(\mathbf{x}) + (1-\varepsilon) f_{ISL}(\mathbf{x}) \right\} \\ s.t. \quad &\left|\mathbf{x}(n)\right| = 1, n = 1,2,\cdots,N. \\ &\left|\mathbf{v}(n)\right| = 1, n = 1,2,\cdots,2N. \end{aligned} \tag{10}$$

Substituting the penalty functions in (6) and (8) into the objective function defined in (10), the design problem can be rewritten as

$$\begin{aligned} &\min \left\{ \varepsilon \left\| \mathbf{S}^H \mathbf{x} \right\|^2 + (1-\varepsilon) \left\| \mathbf{G}^H \mathbf{x} - \sqrt{N} \mathbf{v} \right\|^2 \right\} \\ &s.t. \left| \mathbf{x}(n) \right| = 1, n = 1, 2, \cdots, N. \\ &\quad \left| \mathbf{v}(n) \right| = 1, n = 1, 2, \cdots, 2N. \end{aligned} \tag{11}$$

The optimization problem in (11) is difficult to solve directly because it is a bi-variable optimal problems. Notice that both variable and are only constrained by the same unimodular constraint, so this issue can be addressed by combining the two variables into one variable defined as $\mathbf{y} = \left[\mathbf{x}^T \quad \mathbf{v}^T \right]^T \in C^{3N \times 1}$ .More important, the objective function in (11) is sum of squares of Euclidean norms. With the use of parallelogram identity of Euclidean norms, the following equation is satisfied.

$$\begin{aligned} &\varepsilon \left\| \mathbf{S}^H \mathbf{x} \right\|^2 + (1-\varepsilon) \left\| \mathbf{G}^H \mathbf{x} - \sqrt{N} \mathbf{v} \right\|^2 \\ &= \frac{1}{2} \left\{ \left\| \sqrt{1\text{-}\varepsilon} \mathbf{G}^H \mathbf{x} \text{-} \sqrt{(1\text{-}\varepsilon) N} \mathbf{v} + \sqrt{\varepsilon} \mathbf{S}^H \mathbf{x} \right\|^2 \right. \\ &\quad \left. + \left\| \sqrt{1\text{-}\varepsilon} \mathbf{G}^H \mathbf{x} \text{-} \sqrt{(1\text{-}\varepsilon) N} \mathbf{v} \text{-} \sqrt{\varepsilon} \mathbf{S}^H \mathbf{x} \right\|^2 \right\} \\ &= \frac{1}{2} \left\{ \left\| \mathbf{A}\mathbf{y} \right\|^2 + \left\| \mathbf{B}\mathbf{y} \right\|^2 \right\} \end{aligned} \tag{12}$$

where matrix and are given by

$$\mathbf{A} = \left[\sqrt{1\text{-}\varepsilon} \mathbf{G}^H + \sqrt{\varepsilon} \mathbf{S}^H \quad \text{-} \sqrt{(1\text{-}\varepsilon) N} \mathbf{I}_{2N} \right] \tag{13}$$

$$\mathbf{B} = \left[\sqrt{1\text{-}\varepsilon} \mathbf{G}^H - \sqrt{\varepsilon} \mathbf{S}^H \quad \text{-} \sqrt{(1\text{-}\varepsilon) N} \mathbf{I}_{2N} \right] \tag{14}$$

Thus, the optimization problem (11) can be stated as a compact form.

$$\begin{aligned} &\min \left\{ \left\| \mathbf{A}\mathbf{y} \right\|^2 + \left\| \mathbf{B}\mathbf{y} \right\|^2 \right\} \\ &s.t. \quad \left| \mathbf{y}(n) \right| = 1, n = 1, 2, \cdots, 3N. \end{aligned} \tag{15}$$

3. Algorithm Development

he difficulty lies in the optimization problem (15) is non-convexity caused by unimodular constraint. In this section, the design problem is firstly reformulated to simplify the nonconvex optimization problem. Subsequently, an algorithm is derived based on Alternating Direction Method of Multipliers (ADMM) to solve (15).

3.1. Problem Reformulation

To address the issue of non-convexity in (11), the objective function is split into two terms which consist of a linear term and a quadratic term. Similar to [16], the last element of $\mathbf{y}$ is assigned to be one and define $\mathbf{y}_1 = [\mathbf{y}(1), \mathbf{y}(2), \cdots \mathbf{y}(3\text{N-}1)]_N^T \in {}^{(3N-1)\times 1}$. To relax the unimodular constraint enforced into the quadratic term, an auxiliary unimodular variable vector $\mathbf{z}$ is introduced with the constraint $\mathbf{y}_1 = \mathbf{z}$. Let $\mathbf{y} = \left[\mathbf{y}_1^T \quad 1 \right]^T$, $\mathbf{A} = \left[\mathbf{A}_1 \quad -\sqrt{(1-\varepsilon)N} \mathbf{e}_{2N} \right]$, and $\mathbf{B} = \left[\mathbf{B}_1 \quad -\sqrt{(1-\varepsilon)N} \mathbf{e}_{2N} \right]$ where $\mathbf{A}_1$ and $\mathbf{B}_1$, is composed

of first 3N-1 columns of matrix A and B, respectively. The $\mathbf{e}_{2N}$ represents $2N\times 1$ unit vector with the last element assigned to be one.

The optimization problem (11) can be rewritten as the following equivalent form where the constant terms are removed.

$$\begin{aligned}\min_{y}\Big\{&\mathbf{y}_1^H\mathbf{A}_1^H\mathbf{A}_1\mathbf{y}_1-\sqrt{(1-\varepsilon)N}\mathbf{z}^H\mathbf{A}_1^H\mathbf{e}_{2N}\\&-\sqrt{(1-\varepsilon)N}\mathbf{e}_{2N}^H\mathbf{A}_1\mathbf{z}+\mathbf{y}_1^H\mathbf{B}_1^H\mathbf{B}_1\mathbf{y}_1\\&-\sqrt{(1-\varepsilon)N}\mathbf{z}^H\mathbf{B}_1^H\mathbf{e}_{2N}-\sqrt{(1-\varepsilon)N}\mathbf{e}_{2N}^H\mathbf{B}_1\mathbf{z}\Big\}\\&s.t.\mathbf{y}_1=\mathbf{z}\\&\quad|\mathbf{z}(n)|=1,n=1,2,\cdots,3N-1.\end{aligned}\tag{16}$$

To apply ADMM to the design problem, (16) is further converted to real-valued expression.

$$\begin{aligned}\min_{y}&\left\{\bar{\mathbf{y}}_1^T\mathbf{H}_A\bar{\mathbf{y}}_1+2\mathbf{c}_A^T\bar{\mathbf{z}}+\bar{\mathbf{y}}_1^T\mathbf{H}_B\bar{\mathbf{y}}_1+2\mathbf{c}_B^T\bar{\mathbf{z}}\right\}\\s.t.\quad&\bar{\mathbf{y}}_1=\bar{\mathbf{z}}\\&z_{n,r}^2+z_{n,i}^2=1=1,n=1,2\cdots 3N-1.\end{aligned}\tag{17}$$

where $\bar{\mathbf{y}}_1=[\Re(\mathbf{y}_1^T)\quad\Im(\mathbf{y}_1^T)]^T$, $\bar{\mathbf{z}}=[\Re(\mathbf{z}^T)\quad\Im(\mathbf{z}^T)]^T$. $z_{n,r}$ and $z_{n,i}$ are the real and image part of z_n, respectively. $\mathbf{c}_A$, $\mathbf{c}_B$, $\mathbf{H}_A$ and $\mathbf{H}_B$ are given by

$$\mathbf{c}_A=-\sqrt{(1-\varepsilon)N}\left[\Re(\mathbf{e}_{2N}^T\mathbf{A}_1)\quad-\Im(\mathbf{e}_{2N}^T\mathbf{A}_1)\right]^T\tag{18}$$

$$\mathbf{c}_B=-\sqrt{(1-\varepsilon)N}\left[\Re(\mathbf{e}_{2N}^T\mathbf{B}_1)\quad-\Im(\mathbf{e}_{2N}^T\mathbf{B}_1)\right]^T\tag{19}$$

$$\begin{aligned}\mathbf{H}_A=&\left[\Re(\mathbf{A}_1)\quad-\Im(\mathbf{A}_1)\right]^T\left[\Re(\mathbf{A}_1)\quad-\Im(\mathbf{A}_1)\right]\\&+\left[\Im(\mathbf{A}_1)\quad\Re(\mathbf{A}_1)\right]^T\left[\Im(\mathbf{A}_1)\quad\Re(\mathbf{A}_1)\right]\end{aligned}\tag{20}$$

$$\begin{aligned}\mathbf{H}_B=&\left[\Re(\mathbf{B}_1)\quad-\Im(\mathbf{B}_1)\right]^T\left[\Re(\mathbf{B}_1)\quad-\Im(\mathbf{B}_1)\right]\\&+\left[\Im(\mathbf{B}_1)\quad\Re(\mathbf{B}_1)\right]^T\left[\Im(\mathbf{B}_1)\quad\Re(\mathbf{B}_1)\right]\end{aligned}\tag{21}$$

Let λ and ρ denote the Lagrange multiplier vector and step size respectively, augmented Lagrangian function is devise.

$$\begin{aligned}\mathrm{L}_\rho\left(\bar{\mathbf{y}}_1,\bar{\mathbf{z}},\lambda\right)=&\bar{\mathbf{y}}_1^T\mathbf{H}_A\bar{\mathbf{y}}_1+2\mathbf{c}_A^T\bar{\mathbf{z}}+\bar{\mathbf{y}}_1^T\mathbf{H}_B\bar{\mathbf{y}}_1\\&+2\mathbf{c}_B^T\bar{\mathbf{z}}+\lambda^{\mathrm{T}}\left(\bar{\mathbf{y}}_1-\bar{\mathbf{z}}\right)+\frac{\rho}{2}\left\|\bar{\mathbf{y}}_1-\bar{\mathbf{z}}\right\|_2^2\end{aligned}\tag{22}$$

3.2. Solution to (22)

Algorithm1

Step1: Initialize $\mathbf{y}_1$ with random-phase sequence $\{\mathbf{y}(n)\}_{n=1}^{3N}$, $\boldsymbol{\lambda}$ and ρ.

Step2: Compute $\mathbf{z}(t+1)$ using (25) and (26) with $\mathbf{y}1(t), \boldsymbol{\lambda}(t)$ fixed at most recent value.

Step3: Compute $\mathbf{y}1(t+1)$ using (29) with $\mathbf{z}(t+1), \boldsymbol{\lambda}(t)$ fixed at most recent value.

Step4: Computing $\boldsymbol{\lambda}(t+1)$ using (30).

Step5: Repeat step 2 to 4 until convergence.

In this subsection, an algorithm is proposed for minimizing ISL and stopband power metric based on ADMM. It is briefly summarized as Algorithm 1 consisting of five steps. The three key steps, namely, step 2 to 4, of this algorithm are elaborated further as follows.

Step2: Update with the obtained at the tth iteration.

$$\begin{aligned}\bar{\mathbf{z}}(t+1) &= \arg\min_{\mathbf{z}} \mathrm{L}_{\rho}\left(\bar{\mathbf{y}}_1(t), \bar{\mathbf{z}}, \boldsymbol{\lambda}(t)\right) \\ &= \arg\min_{\bar{z}} \left\{2(\mathbf{c}_A + \mathbf{c}_B)^T \bar{\mathbf{z}} - \boldsymbol{\lambda}^T(t)\bar{\mathbf{z}} - \rho\bar{\mathbf{y}}_1(t)\bar{\mathbf{z}}\right\} \\ s.t. \quad & z_{n,r}^2 + z_{n,i}^2 = 1, n = 1,2,\cdots,3N-1\end{aligned} \tag{23}$$

Since the nonconvex constraint is only enforced on the linear function only, the optimization problem can be simplified by decomposing it into 3N-1 subproblems with variable pair $\{z_{n,r}, z_{n,i}\}$

$$\begin{aligned}&\min \xi_n z_{n,r} + \beta_n z_{n,i} \\ s.t. \quad & z_{n,r}^2 + z_{n,i}^2 = 1, n = 1,2,\cdots,3N-1.\end{aligned} \tag{24}$$

where ξ_n and β_n denote the nth and $(3N\text{-}1+n)$th element of the $2(\mathbf{c}_A + \mathbf{c}_B)^T - \boldsymbol{\lambda}^T(t) - \rho\bar{\mathbf{y}}_1^{\mathrm{T}}(t)$ (24) is a quadratic constraint linear optimization problem, and it can be solved by the Lagrange multipliers method (Readers can refer to more details in [16]). The optimal solution of (24) is given by

$$z_{n,r}(t+1) = -\frac{2\xi_n}{\sqrt{\xi_n^2 + \beta_n^2}} \tag{25}$$

$$z_{n,i}(t+1) = -\frac{2\beta_n}{\sqrt{\xi_n^2 + \beta_n^2}} \tag{26}$$

Step3: Update $\bar{\mathbf{y}}_1$ with the $\left\{\bar{\mathbf{z}}(t+1), \boldsymbol{\lambda}(t)\right\}$ at the most recent value.

$$\begin{aligned}\bar{\mathbf{y}}_1(t+1) &= \arg\min_{\mathbf{y}_1} \mathrm{L}_{\rho}\left(\bar{\mathbf{y}}_1, \bar{\mathbf{z}}(t+1), \boldsymbol{\lambda}(t)\right) \\ &= \arg\min_{\bar{\mathbf{y}}_1} \bar{\mathbf{y}}_1^T \mathbf{H}_A \bar{\mathbf{y}}_1 + \bar{\mathbf{y}}_1^T \mathbf{H}_B \bar{\mathbf{y}}_1 + \\ &\boldsymbol{\lambda}(t)^{\mathrm{T}}\left(\bar{\mathbf{y}}_1 - \bar{\mathbf{z}}(t+1)\right) + \frac{\rho}{2}\left\|\bar{\mathbf{y}}_1 - \bar{\mathbf{y}}(t+1)\right\|_2^2\end{aligned} \tag{27}$$

It is obvious that the analytical solution of (27) can be obtained directly, but computing the (6N-2) matrix inverse is time-consuming and computationally demanding. In order to reduce the computation complexity, (27) is converted from real-valued version into complex-valued version, which is stated as

$$\begin{aligned}&\min_{\mathbf{y}_1}\left\{\mathbf{y}_1^H A_1^H \mathbf{A}_1 \mathbf{y}_1 + \mathbf{y}_1^H \mathbf{B}_1^H B_1 \mathbf{y}_1\right.\\&+\boldsymbol{\lambda}_r(t)^{\mathrm{T}}\left(\Re(\mathbf{y}_1)-\Re(\mathbf{z})\right)+\frac{\rho}{2}\left\|\Re(\mathbf{y}_1)-\Re(\mathbf{z})\right\|_2^2\\&\left.+\boldsymbol{\lambda}_i(t)^{\mathrm{T}}\left(\Im(\mathbf{y}_1)-\Im(\mathbf{z})\right)+\frac{\rho}{2}\left\|\Im(\mathbf{y}_1)-\Im(\mathbf{z})\right\|_2^2\right.\end{aligned} \tag{28}$$

where $\boldsymbol{\lambda}_r(t)$ and $\boldsymbol{\lambda}_i(t)$ represent the first and last (3N-1) elements of . Let $\boldsymbol{\lambda}_c(t)=\boldsymbol{\lambda}_r(t)+j\boldsymbol{\lambda}_i(t)$, the solution to (28) can be computed by

$$\begin{aligned}\mathbf{y}_1(t+1)&=\arg\min_{\mathbf{y}_1} \mathrm{L}_\rho\left(\mathbf{y}_1,\mathbf{z}(t+1),\boldsymbol{\lambda}_{\mathrm{c}}(t)\right)\\&=\arg\min_{\mathbf{y}_1}\left\{\mathrm{y}_1^H\mathbf{A}_1^H\mathbf{A}_1\mathbf{y}_1+\mathbf{y}_1^H\mathbf{B}_1^H\mathbf{B}_1\mathbf{y}_1\right.\\&\left.+\frac{\rho}{2}\left\|\mathbf{y}_1-\mathbf{z}(t+1)+\frac{\boldsymbol{\lambda}_{\mathrm{c}}(t)}{\rho}\right\|_2^2\right\}\\&=\mathbf{J}^{-1}\mathbf{d}(t)\end{aligned} \tag{29}$$

where $\mathbf{J}=\mathbf{A}_1^H\mathbf{A}_1+\mathbf{B}_1^H\mathbf{B}_1+\frac{\rho}{2}\mathbf{I}_{3N-1}$ and $\mathbf{d}(t)=\frac{1}{2}\left(\boldsymbol{\lambda}_{\mathrm{c}}-\rho\mathbf{z}(t+1)\right)$. However, the solution has computation complexity due to the matrix inverse and multiplications required by $\mathbf{J}^{-1}\mathbf{d}(t)$.

Step4: Update using:

$$\boldsymbol{\lambda}(\mathrm{t}+1)=\boldsymbol{\lambda}(t)+\rho\left(\bar{\mathbf{y}}_1(t+1)-\bar{\mathbf{z}}(t+1)\right) \tag{30}$$

Step 1 to 3 are repeated until the convergence condition is satisfied, e.g., $\left\|\mathbf{y}_1(t+1)-\mathbf{z}(t+1)\right\|_2<\delta$ where δ is a predefined threshold.

$$\begin{aligned}&\min\left\{\|\mathbf{A}\mathbf{y}\|^2+\|\mathbf{B}\mathbf{y}\|^2\right\}\\&s.t.\quad |\mathbf{y}(n)|=1, n=1,2,\cdots,3N.\end{aligned} \tag{15}$$

4. Numerical Simulation

In this section, several numerical results are presented to demonstrate the effectiveness of two proposed algorithms. We first investigate the performance of Algorithm 1 which aims to design sequence for single-input and single-output (SISO) radar. The second example aims to analyze how the relative weight affect the performance of algorithm 1. The third example is conducted to assess the performance of Algorithm 2. All simulations were conducted on a PC with a 3.20GHz i7 CPU and 64GB RAM using MATLAB R2018b.

In the first example, we design the unimodular sequence with length of 128 for SISO radar. The proposed algorithm is compared with the state-of-the-art algorithms that of SCAN [9] and spectral-MISL(SMISL) [11]. For fair comparison, the relative weight of all the algorithms is assigned to make the ISL of waveform produced by each algorithm almost the same. The is assigned in the proposed and SCAN algorithm, and the trade-off parameter in SMISL is tuned as 500. Additionally, the normalized spectral stopband locates in for all algorithms, which is the same as the stopband specified in [9]. The stopping criterion is set to be $\left\|\mathbf{x}_k-\mathbf{x}_{k+1}\right\|_2<$ 1e-5. We produce 500 sequences initialized by random-phase sequence, and use the same initial sequences in all algorithms.

We investigate the correlation and stopband properties for the tested algorithms, and then conduct their performance evaluations in terms of the following characteristics: i) the PSL and ISL values of the produced sequence when the algorithms reach the preset convergence condition; ii) P_{stop} defined as $P_{\text{stop}} = 10\log_{10}(\max|Y(k)|^2)$, where $Y(k)$ denotes the 2N-points FFT of the designed sequence; iii) average passband-to-stopband power ratio (APSPR) [12],[33], that is

$$\text{APSPR}=10\log_{10}\left(\frac{P_{\text{p}}/N_{\text{p}}}{P_{\text{s}}/N_{\text{s}}}\right) \tag{31}$$

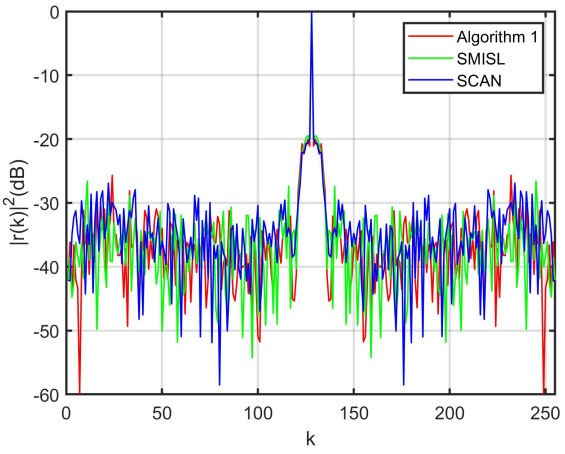

(a)

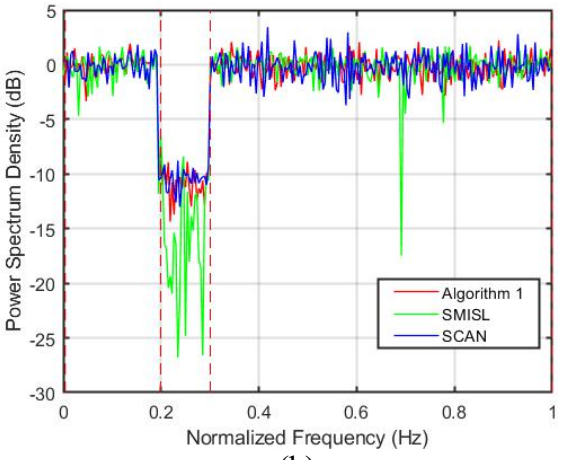

(b)

Figure 1: Comparison of one simulation result produced by Algorithm 1, SMISL and SCAN. (a) autocorrelations; (b) power spectrum density.

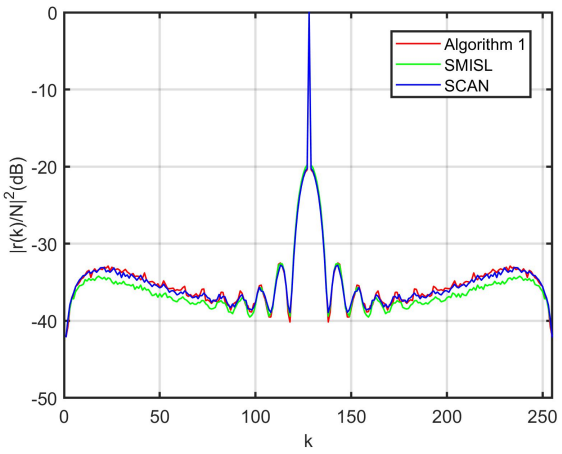

Figure 2: Comparison of average autocorrelations of 500 independent simulation results produced by Algorithm 1, SMISL and SCAN.

Table 1: Peromace Comparison of Three Algorithms.

Method	**ISL[dB]**	**PSL[dB]**	P_{stop} **[dB]**	**APSPR[dB]**
Algorithm1	-8.056	-20.081	-8.921	-10.653
SCAN	-7.773	-20.735	8.781	-10.401
SMISL	-7.268	-19.452	-8.408	-13.103

where P_p and P_s are the total power in the passband and stopband, respectively. N_p and N_s represent the number of frequencies in passband and stopband.

Figure 1 shows autocorrelation and power spectrum density of the sequence of one simulation result, and performance comparison is listed in Table I. It can be seen from the Figure 1(a) that for all tested algorithms, the performance is comparable in terms of PSL. The normalized PSL values of Algorithm 1, SCAN and SMISL are -20.081 dB, -20.735 dB, and -19.425 dB, respectively. Among all the tested algorithms, the proposed algorithm produce sequence with the lowest ISL P_{stop} and as shown in Table 1. As far as APSPR, the SMISL is most attractive, and the algorithm 1 is better than SCAN. In addition, Figure 1(b) shows that sequence produced by algorithm 1 jitters least. Analyzing of the results verifies that Algorithm 1 can produce sequence with the best correlation and P_{stop} performance under some certain initial sequences.

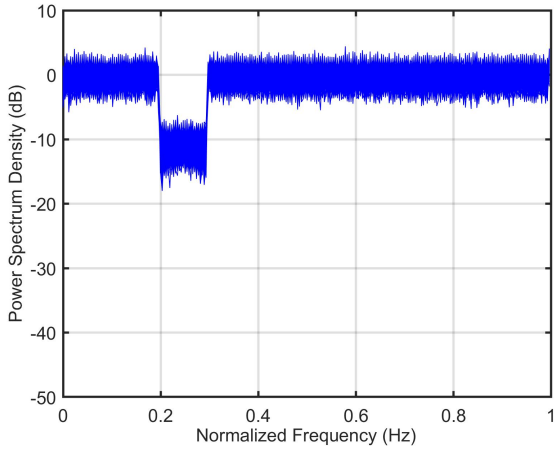

Figure 3: Power spectrum density of 500 simulation results produced by Algorithm 1.

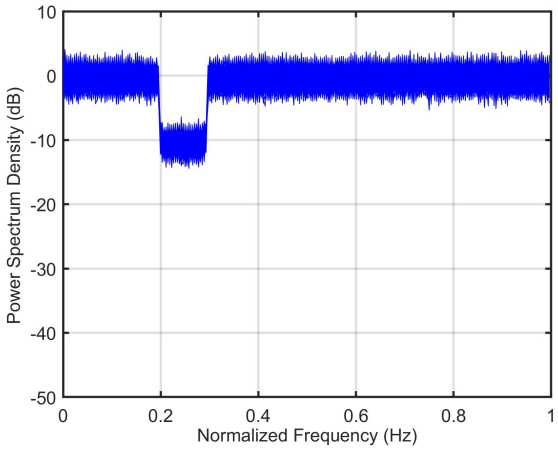

Figure 4: Power spectrum density of 500 simulation results produced by SCAN.

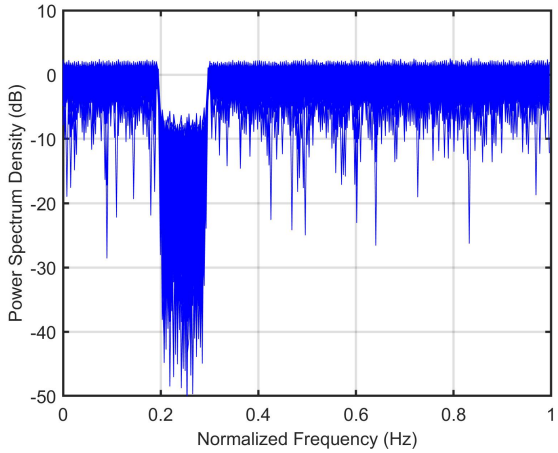

Figure 5: Power spectrum density of 500 simulation results produced by SMISL.

Table 1: Average of ISL and APSPR.

Method	ISL[dB]	APSPR[dB]
Algorithm1	-7.776	-10.832
SCAN	-7.835	-10.303
SMISL	-7.952	-13.564

The performance comparison is conducted further based on the 500 simulation results. Figure 2 shows the average aperiodic normalized autocorrelation of 500 independent results, and the average values of ISL are listed in Table II. Corresponding to Algorithm 1, SMISL and SCAN, the average values of ISL are -7.776 dB, -7.952 dB and -7.835 dB. Thus, all the tested algorithms have comparable autocorrelation performance in the first example. The normalized power spectrum density of Algorithm 1, SCAN and SMISL is plotted in Fig.3 to 5, and their average APSPR values are -10.832 dB, -10.303 dB and -13.564 dB, as listed in Table II. From the Figure 3 to 5, it is apparent that sequences produced by Algorithm 1 and SCAN jitter less than SMISL in the passband.

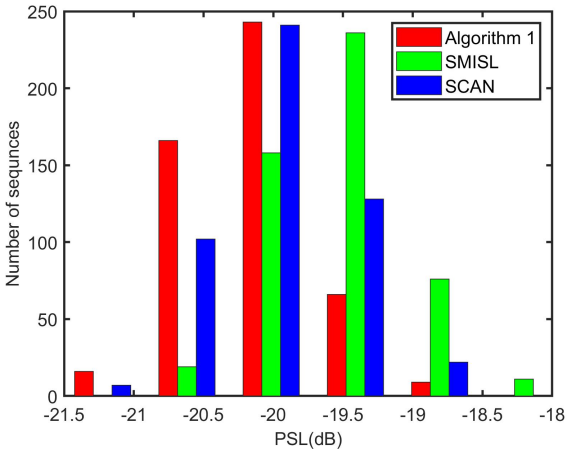

Figure 6: PSL distribution of 500 simulation results produced by tested algorithms.

To further evaluate the performance of power spectrum density and autocorrelation, we analyze the distributions of P_{stop} and PSL of all sequences produced by the tested algorithms, and plot them in Fig. 6 and 7. As shown in Fig. 6, the PSL of most sequences obtained from proposed algorithm, i.e., 85%, have magnitudes less than -19.75 dB. It can be seen from Fig.7 that more sequences produced by the proposed algorithm and SCAN, corresponding to 93.4% and 95%, have P_{stop} less than -7.5 dB, though the SMISL get better performance in terms of APSPR.

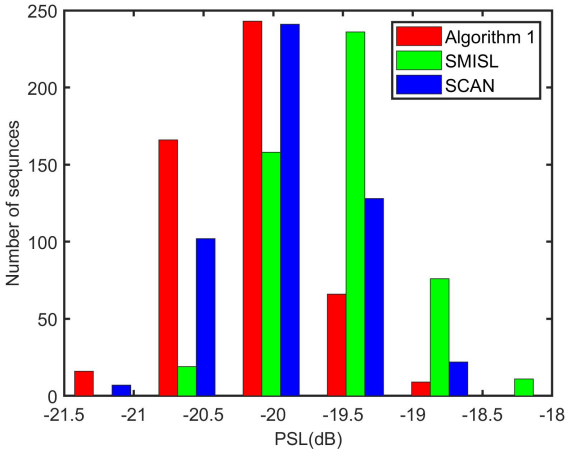

Figure 7: Peak stopband power distribution of 500 simulation results produced by tested algorithms.

This example demonstrates the effectiveness of the proposed algorithm of designing sequence with good correlations and suppressed stopband power. Form the discussion above, the following findings are obtained. i) Simulation results presented in Fig.6 shows that the proposed algorithm is best among the tested algorithms in terms of ISL; ii) With ISL being the same, the proposed algorithm is better than SMISL in terms of P_{stop} and spectral flatness, and almost the same as SCAN; iii) As far as APSPR, the SMISL is most attractive, and algorithm 1 is better than SCAN. Hence, the proposed algorithm may turn out to be a good choice when all autocorrealtion and spectrum characteristics are considered.

In the second example, the algorithm performance is evaluated versus different relative weight ε, and the SCAN algorithm is tested for comparison. The SMISL algorithm is excluded because its tradeoff parameter is different from the proposed algorithm and needs to adjust with the change of relative weight of proposed algorithm. The relative weight is increased from 0.1 to 0.9, namely, $\varepsilon \in \{0.1, 0.2, 0.3,\ 0.4, 0.5, 0.6, 0.7, 0.8, 0.9\}$ Similarly, we produce 100 ε independent sequences for each in this example. The tested algorithms are initialized by the same random-phase sequence set. The remaining parameters are identical to those in the first example.

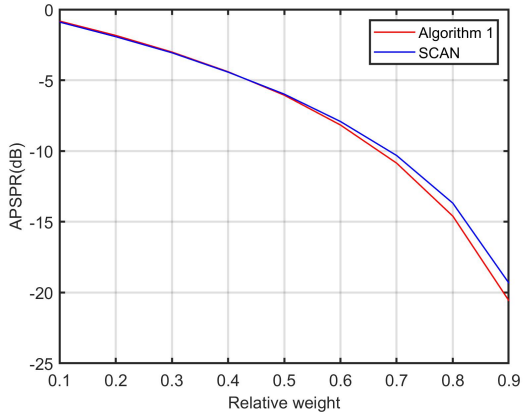

Figure 8: Comparison of average APSPR of 100 sequences versus relative weight.

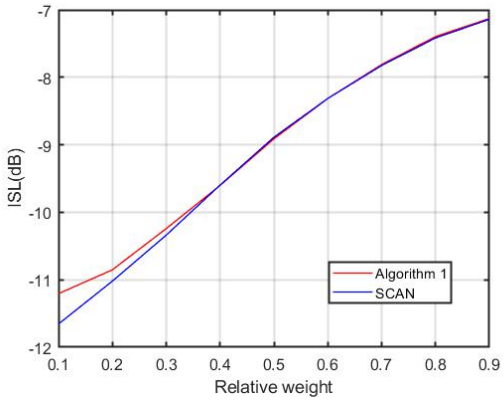

Figure 9: Comparison of average ISL of 100 sequences versus relative weight.

The ISL and APSPR versus different relative weight are plotted in Figure 8 and 9. As can be seen from Figure 8 and 9, APSPR of both algorithms decrease with the increase of relative weight, and ISL shows the opposite trend.

The proposed algorithm produces sequences with lower APSPR than SCAN when relative weight $\varepsilon < 0.5$, whereas both algorithms are almost the same in terms of ISL. When relative weight $\varepsilon > 0.5$, the proposed algorithm is inferior to SCAN in terms of ISL with almost identical APSPR. The results of this example indicate that the proposed algorithm is better when we focus far more on APSPR, and SCAN performs better when ISL is more critical.

5. Conclusions

In this paper, we consider unimodular sequence design problem under the spectral and correlation sidelobe constraints, which is formulated as a bi-objective optimization problem subject to unimodular constraint. The optimization problem is further simplified as a single objective optimization problem based on Pareto optimization method and parallelogram identity. By introducing an auxiliary variable, the non-convex and NP-hard problem is separated into a linearly constrained quadratic program and an unimodular constrained linear program. An algorithm is developed based on ADMM framework to find the Pareto-optimal solution of the design problem. Simulation results demonstrate the effectiveness of the proposed algorithms.

A limitation of this study is that the proposed algorithm shows slower convergence rate than the state-of-the-art algorithms. As future work, we will focus on simplify the computation complexity further in the computationally demanding steps and accelerate the convergence of algorithm. In addition, it might be interesting to synthesize sequence set with flat spectrum, i.e. designing unimodular orthogonal sequence set under specified spectral shape and unimodular constraint.

References

[1] L. Wu, P. Babu, and D. P. Palomar, "Transmit waveform/receive filter design for MIMO radar with multiple waveform constraints," IEEE Trans. Signal Process., vol. 66, pp. 1526–1540, Mar. 2018.

[2] J. H. He, J. Li, and P. Stoica, Waveform design for active sensing systems: A computational approach. Cambridge, U. K.: Cambridge Univ. Press, 2012.

[3] M. J. Lindenfeld, "Sparse frequency transmit-and-receive waveform design," IEEE Trans. Aerosp. Electron. Syst., vol. 40, no. 3, pp. 851–861, July 2004.

[4] I. W. Selesnick and S. U. Pillai, "Chirp-like transmit waveforms with multiple frequency-notches," in IEEE Radar Conf., May 2011, pp. 1106–1110.

[5] K. Gerlach, M. R. Frey, M. J. Steiner, and A. Shackelford, "Spectralnulling on transmit via nonlinear FM radar waveforms," IEEE Trans.Aerosp. Electron. Syst., vol. 47, no. 2, pp. 1507–1515, April 2011.

[6] S. Blunt, M. Cook, J. Jakabosky, J. De Graaf, and E. Perrins, "Polyphasecoded FM (PCFM) radar waveforms, part i: Implementation," IEEE Trans. Aerosp. Electron. Syst., vol. 50, pp. 2218–2229, Jul 2014.

[7] S. Blunt, J. Jakabosky, M. Cook, J. Stiles, S. Seguin, and E. Mokole, "Polyphase-coded FM (PCFM) radar waveforms, part ii: optimization," IEEE Trans. Aerosp. Electron. Syst., vol. 50, no. 3, pp. 2230–2241, Jul 2014.

[8] D. Zhao, Y. Wei, and Y. Liu, "PCFM radar waveform design with spectral and correlation considerations," IEEE Trans. Aerosp. Electron. Syst., vol. 53, no. 6, pp. 2885–2898, Dec 2017.

[9] H. He, P. Stoica, and J. Li, "Waveform design with stopband and correlation constraints for cognitive radar," in Proc. 2nd Int. Workshop on Cogn. Inf. Process. (CIP), June 2010, pp. 344–349.

[10] G. Cui, X. Yu, A. G. Yang, and L. Kong, "Cognitive phase-only sequence design with desired correlation and stop-band properties," IEEE Trans. Aerosp. Electron. Syst., vol. PP, no. 99, pp. 1–1, 2017.

[11] J. Song, P. Babu, and D. P. Palomar, "Optimization methods for designing sequences with low autocorrelation sidelobes," IEEE Trans. Signal Process., vol. 63, no. 15, pp. 3998–4009, Aug 2015.

[12] W. Guohua, M. Chaoyun, S. Jinping, and L. Yilong, "Sparse frequency waveform analysis and design based on ambiguity function theory," IET Radar, Sonar Navig., vol. 10, no. 4, pp. 707–717, 2016.

[13] L. Tang, Y. Zhu, H. Wu, and Q. Fu, "Fast algorithms for sparse frequency waveform design with sidelobe constraint," Digit. Signal Process., vol. 69, pp. 140–153, 2017.

[14] W. Rowe, P. Stoica, and L. Jian, "Spectrally constrained waveform design," IEEE Signal Process. Mag., vol. 31, no. 3, pp. 157–162, 2014.

[15] J. Liang, H. C. So, C. S. Leung, J. Li, and A. Farina, "Waveform design with unit modulus and spectral shape constraints via lagrange programming neural network," IEEE J. Sel.Topics Signal Process., vol. 9, no. 8, pp. 1377–1386, Dec 2015.

[16] J. Liang, H. C. So, J. Li, and A. Farina, "Unimodular sequence design based on alternating direction method of multipliers," IEEE Trans. Signal Process., vol. 64, no. 20, pp. 5367–5381, Oct 2016.

[17] Y. Jing, J. Liang, D. Zhou, and H. C. So, "Spectrally constrained unimodular sequence design without spectral level mask," IEEE Signal Process. Lett., vol. 25, pp. 1004–1008, Jul. 2018.

[18] G. Cui, H. Li, and M. Rangaswamy, "MIMO radar waveform design with constant modulus and similarity constraints," IEEE Trans. Signal Process., vol. 62, no. 2, pp. 343–353, Jan. 2014.

[19] Z. Cheng, Z. He, B. Liao, and M. Fang, "MIMO radar waveform design with PAPR and similarity constraints," IEEE Trans. Signal Process., vol. 66, no. 4, pp. 968–981, Feb 2018.

[20] H. He, P. Stoica, and J. Li, "Designing unimodular sequence sets with good correlations—including an application to MIMO radar," IEEE Trans. Signal Process., vol. 57, no. 11, pp. 4391–4405, Nov 2009.

[21] Z. Wang, P. Babu, and D. P. Palomar, "Design of PAR-constrained sequences for MIMO channel estimation via majorization– inimization," IEEE Trans. Signal Process., vol. 64, no. 23, pp. 6132–6144, Dec 2016.

[22] A. Aubry, A. De Maio, B. Jiang, and S. Zhang, "Ambiguity function shaping for cognitive radar via complex quartic optimization," IEEE Trans. Signal Process., vol. 61, no. 22, pp. 5603–5619, Nov 2013.

[23] Y. Jing, J. Liang, B. Tang, and J. Li, "Designing unimodular sequence with low PSL of local ambiguity function," IEEE Trans. Aerosp. Electron. Syst., vol. PP, pp. 1–1, 09 2018.

[24] N. Parikh and S. Boyd, "Proximal algorithms," Found. Trends Optim., vol. 1, no. 3, pp. 123–231, 2013.

[25] Z. Cheng, Z. He, S. Zhang, and J. Li, "Constant modulus waveform design for MIMO radar transmit beampattern," IEEE Trans. Signal Process., vol. 65, no. 18, pp. 4912–4923, Sep. 2017.

[26] H. Ji, W. Yu, and Y. Li, "A rank revealing randomized singular value decomposition (R3SVD) algorithm for low-rank matrix pproximations," Comput. Res. Repository, 05 2016.

[27] Z. Jia and y. yang, "Modified truncated randomized singular value decomposition (MTRSVD) algorithms for large scale discrete ill-posed problems with general-form regularization," Inverse Problems, vol. 34, 03 2018.

[28] P. Stoica, H. He, and J. Li, "New algorithms for designing unimodular sequences with good correlation properties," IEEE Trans. Signal Process., vol. 57, no. 4, pp. 1415–1425, April 2009.

[29] H. Esmaeili-Najafabadi, M. Ataei, and M. F. Sabahi, "Designing sequence with minimum PSL using chebyshev distance and its application for chaotic MIMO radar waveform design," IEEE Trans. Signal Process., vol. 65, no. 3, pp. 690–704, Feb 2017.

[30] M. A. Kerahroodi, A. Aubry, A. De Maio, M. M. Naghsh, and M. Modarres-Hashemi, "A coordinate-descent framework to design low PSL/ISL sequences," IEEE Trans. Signal Process., vol. 65, no. 22, pp. 5942–5956, Nov. 2017.

[31] Y. Li and S. A. Vorobyov, "Fast algorithms for designing multiple unimodular waveforms with good correlation properties," IEEE Trans. Signal Process., vol. PP, no. 99, pp. 1197–1212, 2017.

[32] G. Wang and Y. Lu, "Designing single/multiple sparse frequency waveforms with sidelobe constraint," IET Radar, Sonar Navig., vol. 5, no. 1, pp. 32–38, Jan. 2011.

[33] G. Wang and Y. Lu, "Bounds on generalised integrated sidelobe level in waveforms with stopbands," Electron. Lett., vol. 46, no. 23, pp. 1561– 1562, 2010.